

pubs.acs.org/ac Article

# Quantification of Nitric Oxide in Single Cells Using the Single-Probe Mass Spectrometry Technique

Yunpeng Lan, Xingxiu Chen, and Zhibo Yang\*



Cite This: Anal. Chem. 2023, 95, 18871–18879



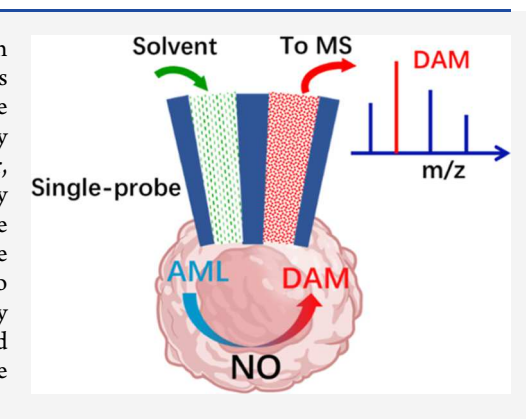
**ACCESS** I

III Metrics & More

Article Recommendations

Supporting Information

ABSTRACT: Nitric oxide (NO) is a small molecule that plays important roles in biological systems and human diseases. The abundance of intracellular NO is tightly related to numerous biological processes. Due to cell heterogeneity, the intracellular NO amounts significantly vary from cell to cell, and therefore, any meaningful studies need to be conducted at the single-cell level. However, measuring NO in single cells is very challenging, primarily due to the extremely small size of single cells and reactive nature of NO. In the current studies, the quantitative reaction between NO and amlodipine, a compound containing the Hantzsch ester group, was performed in live cells. The product dehydro amlodipine was then detected by the Single-probe single-cell mass spectrometry technique to quantify NO in single cells. The experimental results indicated heterogeneous distributions of intracellular NO amounts in single cells with the existence of subpopulations.



# INTRODUCTION

In life processes, bioactive small molecules play critical roles, such as cell signaling, regulation of enzyme activities, and treatment of diseases. Among all bioactive small molecules, nitric oxide (NO) is particularly important, and its production and abundance are tightly relevant to many physiological and pathological processes. NO is a signaling molecule regulating cell survival and proliferation in diverse biological systems. For example, in the cardiovascular system, NO regulates blood flow and blood pressure. The recognition of its role as a cardiovascular signaling molecule has been awarded the 1998 Nobel Prize in Physiology or Medicine. 1,4–7

In a biological system, NO can be produced from exogenous (i.e., provided by NO donor compounds) and endogenous (i.e., produced by cells) resources. Exogenous NO donor compounds have been applied to the treatment of heart and blood pressure-related diseases. For example, nitroglycerin (or glyceryl trinitrate) and sodium nitroprusside (SNP) contain NO in their structures, and they release NO through cell metabolism; they are widely used for the treatment of high blood pressure and heart failure. Hold Endogenous NO can be generated by cells through the catalytical reaction of the NO synthases (NOSs, a family of enzymes catalyzing the production of NO). For example, the anticancer drug doxorubicin (DOX) can promote the activities of NOSs, resulting in increased NO abundances in cells.

The production and abundance of NO are tightly relevant to human health and diseases. For example, in the immune system, low concentrations of NO produce anti-inflammatory effects by inhibiting the proliferation of T helper cells; however, high concentrations of NO lead to strong proinflammatory responses under abnormal conditions.  $^{16-20}$ 

Similarly, the concentration of NO directly influences the angiogenesis in tumors: low concentrations of NO promote the growth and nutrition of tumors due to the formation of blood vessels, whereas high abundances of NO can suppress tumor growth. <sup>21,22</sup> Previous studies showed that the NO level in cancer cells changed after the anticancer drug treatment. <sup>23,24</sup> Therefore, monitoring the abundance of NO in cells is important for both fundamental biological sciences and human diseases.

The abundance of NO in tumors can significantly vary from cell to cell. Factors affecting its intracellular abundances include intrinsic cell heterogeneity, variances in the expression of NOSs,<sup>25</sup> and heterogeneity in the immune response.<sup>26</sup> Cell heterogeneity has been observed in most biological systems and multiple human diseases, such as cancer. Particularly, cell heterogeneity is regarded as a major challenge for cancer studies and treatment.<sup>27,28</sup> Due to cell heterogeneity, NO levels in different single cells significantly vary.<sup>20,29,30</sup> However, quantitative measurement of NO in single cells is very challenging, primarily due to its extremely short lifetime (<1

Received: September 28, 2023 Revised: November 29, 2023 Accepted: December 4, 2023 Published: December 13, 2023





s) and low amounts  $(10^{-19} \text{ mol})$  in single cells with extremely small volumes and very complex cellular species.<sup>31</sup>

A variety of different methods have been developed for quantitative analysis of intracellular NO. These analytical techniques include fluorescence,<sup>32–34</sup> colorimetric,<sup>32,35–3</sup> chemiluminescence, <sup>38-40</sup> electrochemical, <sup>41-43</sup> gas chromatography, 44,45 electron paramagnetic or spin resonance (EPR or ESR), 46-49 and magnetic resonance imaging (MRI). 50,51 Among these methods, fluorescence-based techniques are commonly used, and some of them have been adopted in studies of single cells. 52,53 Because NO cannot directly produce fluorescence, probes [e.g., 2,3-diaminonaphthaline (DAN)] are needed to react with NO and produce fluorescent products for detection.<sup>54</sup> However, fluorescence-based methods have several drawbacks, including interference of cellular autofluorescence and side reactions of NO with other species.<sup>54</sup> In addition, these techniques are unable to detect nonfluorescent molecules, limiting their applications to study broader ranges of cellular species.

Mass spectrometry (MS) is a powerful tool to sensitively detect and accurately identify molecules at low abundances in a complex matrix.<sup>55–57</sup> Recent developments in MS have led to the creation of a variety of different single-cell MS (SCMS) methods. Based on their sampling and ionization conditions, these SCMS techniques can be generally classified into two groups: vacuum-based and ambient methods.<sup>58-61</sup> Vacuumbased methods require a high vacuum environment during analysis and complex sample preparation, but their sensitivity and throughput are relatively higher. Matrix-assisted laser desorption/ionization (MALDI) and secondary ion MS (SIMS) are two widely applied methods for SCMS and MS imaging (MSI). $^{61-64}$  To overcome certain drawbacks of vacuum-based methods, numerous ambient SCMS techniques have been developed. These methods include desorption electrospray ionization (DESI), 65,66 nanospray desorption electrospray ionization (nano-DESI),67-69 video-MS,70-72 Single-probe, 73-75 T-probe, 76,77 laser ablation electrospray ionization (LAESI), 78,79 and pulsed direct current electrospray ionization MS (Pico-ESI-MS).80,81

MS is widely used for the quantitative analysis of cellular compounds such as metabolites and proteins. 82,83 In relatively quantification experiments, the intensities of ions of interest are commonly normalized to the total ion intensity (TIC) for comparison.<sup>84</sup> This method has been often used in SCMS studies due to its convenience. 73,84 Another strategy for relative quantification is to add an internal standard with a fixed concentration into all samples, and the intensities of all target ions are then normalized to that of the internal standard. 85 In absolute quantification studies, internal standard spiking and standard addition are generally used. When the isotopically labeled compound is used as the internal standard, the target compound, which has the same structure as the internal standard, can be quantified without using any calibration curve. 86,87 However, due to the complexity of biological systems, isotopically labeled internal standards for multiple target molecules may not be conveniently available. Therefore, using unlabeled internal standards (e.g., analogues with structures similar to the target molecules) and calibration curves of target molecules is an effective approach to absolute quantification.<sup>22</sup> Standard addition is another strategy, in which a series of samples containing different amounts of the standard are prepared. Based on the response curve, the

absolute abundance of the target molecule can be determined  $^{88}$ 

Quantitative measurement of analytes in single cells is very challenging, primarily due to their extremely limited sizes and complex compositions. Only a few SCMS techniques have been developed for absolute quantification of molecules in single cells. Yin et al. used an electroosmotic extraction method to quantitatively extract Allium cepa cell and internal standard (glucose- $d_2$  solution) into a nanopipette for MS analysis. <sup>89</sup> Our group has developed quantitative Single-probe SCMS methods to measure the absolute abundances and concentrations of anticancer drugs in single cells. 86,87,90 The Single-probe is a miniaturized, multifunctional device for in situ sampling and real-time MS analysis. To fabricate a Single-probe, a solventproviding fused silica capillary and a nano-ESI emitter are embedded into two channels of a dual-bore quartz needle, which is laser-pulled to form a sharp tip ( $\sim$ 10  $\mu$ m). During our routine SCMS analysis, the Single-probe tip is inserted into the target cell to extract cellular contents by a liquid junction of the solvent (e.g., acetonitrile with 1% formic acid) formed on the tip. The extracted cellular contents are spontaneously drawn to the nano-ESI emitter through a self-aspiration process. In quantitative Single-probe SCMS experiments, the internal standard (e.g., an isotopically labeled compound) is added to the solvent with a known concentration. The extracted target molecules in single cells are simultaneously ionized along with the internal standard for MS detection. 91,5

The quantitative Single-probe SCMS experiments have been conducted for both adherent and suspended cells. For adherent cells, a glass chip containing microwells (diameter: 55  $\mu$ m; depth: 25  $\mu$ m) was used as a substrate for cell culture.<sup>86</sup> During the experiments, only single cells inside single microwells were analyzed. The microwells were able to minimize the diffusion loss of molecules, including cellular contents, the target molecules (e.g., anticancer drug irinotecan absorbed the cell), and the internal standard (e.g., irinotecan $d_{10}$ ), to ensure accurate quantification. <sup>86</sup> To analyze suspended cells, an integrated cell manipulation platform was coupled to the Single-probe SCMS setup. A single cell was captured using a cell-selection probe connected to a microinjection, which was used to provide a gentle suction for cell capture, and moved to the Single-probe tip.<sup>87</sup> The liquid junction of the sampling solution (e.g., acetonitrile containing isotopically labeled drug compound) formed on the probe tip immediately lysed the captured cell, and the single cell lysate was then analyzed by MS in real-time to obtain drug quantity. In order to determine the concentration of target molecules (e.g., anticancer drug), cell images were taken during cell selection to estimate the volume of each target.87

To the best of our knowledge, there are no reported studies using the MS method to quantify NO from single cells. Due to NO's small molecular weight, high reactivity, and dissuasive properties, it is challenging to directly analyze this molecule using MS-based methods. Detecting NO from live single cells is more challenging because of its limited amount in each cell. Alternatively, chemical reactions have been used for the indirect MS detection of NO. It has been reported that Hantzsch ester can react with NO with high efficiency and specificity. 93–96 Using amlodipine (AML), a compound containing Hantzsch ester group, 97 NO can efficiently (~100%) and rapidly (<1 s) react with AML to produce dehydro amlodipine (DAM), a stable compound that can be sensitively detected by MS (Figure 1A). 22 Because this

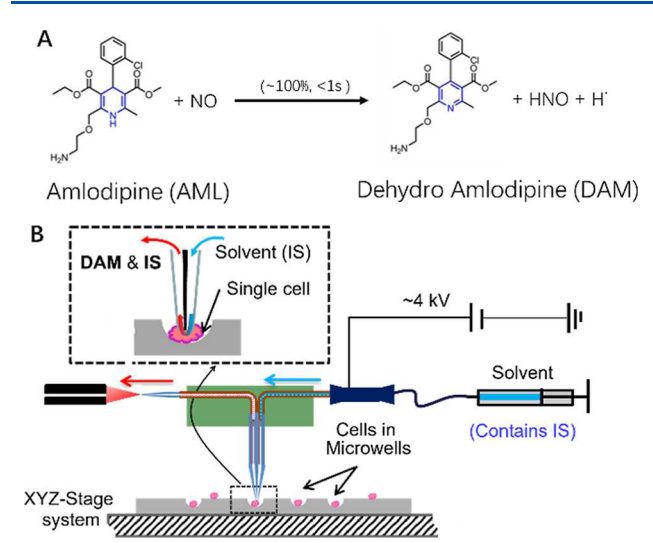


**Figure 1.** Quantification of NO in single cells. (A) Reaction of AML and NO producing DAM. (B) Quantitative Single-probe SCMS cell setup. A Glass chip containing microwells is used for cell culture and the SCMS experiment.

reaction efficiency is nearly 100%, <sup>22</sup> NO can be quantified by measuring the amount of DAM produced from this reaction. <sup>22</sup> These studies also demonstrated that AML does not react with other reactive cellular species (e.g., reactive oxygen and nitrogen species as well as biological reductants) to produce DAM. <sup>22</sup> The integration of the SCMS technique with chemical reactions has been utilized in our previous studies of locating carbon double (C=C) bonds in unsaturated lipids. <sup>98</sup> In the current study, we combined the quantitative Single-probe SCMS technique with the above chemical reaction (Figure 1) to quantitatively measure the amounts of NO in single cells.

# EXPERIMENTAL SECTION

**Experimental Materials and Instruments.** All data were obtained using a Thermo LTQ Orbitrap XL mass spectrometer (Thermo Scientific, Waltham, MA, USA). DAM extracted from cell lysates was analyzed using nanoACQUITY ultraperformance liquid chromatography (LC) (Waters, Milford, MA, USA) coupled to the Orbitrap mass spectrometer.

Chemicals: amlodipine (AML, Cayman Chemical, MI, USA); dehydro amlodipine (DAM, Santa Cruz Biotech, TX, USA); oxasulfuron (OXF, internal standard for SCMS quantification of DAM);  $d_4$ -AML (internal standard for LC–MS quantification of DAM, Cayman Chemical, MI, USA); sodium nitroprusside (SNP, Cayman Chemical, MI, USA); and doxorubicin (DOX, Alfa Aesar, MA, USA).

**Cell Culture.** Human colon cancer cells (HCT-116) were originally obtained from the American Type Culture Collection (ATCC; Rockville, MD, USA). The cell culture medium for HCT-116 is McCoy's 5A cell culture medium containing 10% FBS (fetal bovine serum) and 1% Pen Strep (Life Technologies, Grand Island, NY, USA). All cells were cultured at 37 °C in an incubator with a 5% CO<sub>2</sub> supply (HeraCell, Heraeus, Germany). To prepare cells for SCMS experiments, cells were seeded in 12-well plates ( $5.0 \times 10^5/\text{mL}$  with 2 mL/well) containing microwell glass chips. To prepare cells for LC/MS experiments, cells were seeded in Petri dishes (10 mL/dish) 12 h prior to the drug treatment. AML (dissolved in DMSO) was added into the culture medium (with a final concentration of  $2.0 \ \mu\text{M}$  AML) to treat the cells

for 2 h, and then the medium was disposed of. Cells were washed with PBS two times, and the prepared culture medium containing SNP (exogenous group) or DOX (endogenous group) was used to treat cells for 24 h. Cells were then rinsed with fresh cell culture medium prior to direct SCMS experiments. In addition, rinsed cells were used for lysate preparation and DAM extraction, followed by LC/MS analysis. Cells in control groups, which were treated with AML (without SNP or DOX), SNP (without AML), or DOX (without AML), were used to determine if DAM is solely produced from the reaction between AML and exogenous or endogenous NO.

**Single-Probe SCMS.** The Single-probe is a multifunctional sampling and ionization device. A Single-probe is fabricated by integrating three major components: a needle pulled from dual-bore quartz tubing (outer diameter (o.d.) 500  $\mu$ m; inner diameter (i.d.) 127  $\mu$ m; tip size <10  $\mu$ m; Friedrich & Dimmock, Inc., Millville, NJ, USA) using a laser pipet puller (P-2000 micropipette puller, Sutter Instrument, Novato, CA, USA), a fused silica capillary (o.d. 105  $\mu$ m; i.d. 40  $\mu$ m; Polymicro Technologies, Phoenix, AZ, USA), and a nano-ESI emitter produced using the same type of fused silica capillary. Detailed description of the device fabrication and utilization has been reported in our previous studies.<sup>73–75,86,91</sup> Mass spectrometer settings include the ionization voltage of 4.5 kV, mass resolution of 60,000 (at m/z 400), isolation window of 1 m/z, CID of 20 normalized collision energy (NCE), and mass range from m/z 100-450. The sampling solution used in SCMS experiments was acetonitrile (ACN) containing 0.1% formic acid (FA) and 1.0  $\mu$ M OXF, and the optimized flow rates range between 0.1 and 0.3  $\mu$ L/min in each experiment.

LC/MS. After the used medium was disposed of, cells were washed with PBS. Two mL aliquot of 0.5% trypsin was used to detach cells for 3 min, and trypsinization was stopped by adding 8 mL of culture medium. Cells were centrifuged at 1000 rpm for 5 min, resuspended by PBS for washing, and then counted (Bio-Rad TC20 cell counter, USA). To prepare the cell pellet, cells were centrifuged at 1500 rpm for 5 min. After discarding the supernatant, 200  $\mu$ L Tris buffer (pH = 8.0) containing 8 M urea was added to the cell pellet. The mixtures were sonicated for 20 s (FS-300N, Edeardda; with 50% power) and shaken (with an ice bath) by orbital shaking for 5 min at 100 rpm. To precipitate proteins and extract DAM, 800  $\mu$ L cold acetone (-20 °C) was added into the cell lysate prior to overnight storage (-20 °C). Stored samples were centrifuged at 12,300 rpm at 4 °C for 5 min, and the supernatant was collected to another Eppendorf tube and dried at room temperature using a SpeedVac (SPD111 V, Thermo Scientific, San Jose, CA, USA). The dried samples were resuspended in 200 μL of methanol/water solution [methanol  $(20\%)/H_2O$  (80%) with 0.1% FA]. To desalt samples, 10  $\mu$ L C18 desalting tips (PureSpeed, Rainin Pipetting 360°, Oakland, CA, USA) were used following the vendor's protocols. The eluted solutions were dried by the SpeedVac, and the dried samples were resuspended in 90  $\mu$ L of solution [MeOH (20%)/H<sub>2</sub>O (80%) with 0.1% FA] and 10  $\mu$ L of internal standard (100 nM  $d_4$ -AML).

Home-packed trap column (150  $\mu$ m, 50 mm, 3  $\mu$ m, 100 Å; Daisogel, Japan) and C18 capillary column (150  $\mu$ m, 150 mm, 3  $\mu$ m, 100 Å; Daisogel, Japan) were used for LC separation. Mobile phases A (ACN containing 0.1% FA) and B (H<sub>2</sub>O containing 0.1% FA) were sonicated for 30 min to remove the gas before use. During the analysis, 2  $\mu$ L of the sample was

injected into the trap column, followed by 5 min trapping using 5% mobile phase B at a flow rate of 3  $\mu$ L/min. Separation was performed in the analytical column at a flow rate of 500 nL/min and a column temperature of 50 °C. LC gradient started from 5% mobile phase B for the first 1 min, followed by a quick increase to 45% mobile phase B in 5 min. In the next 12 min, the percentage of mobile phase B was increased to 95% and held for another 5 min. Then, the gradient of mobile phase B was changed back to 5% for 10 min re-equilibrium. The outlet of the analytical column was connected to a nanoESI emitter. The MS analysis parameters are listed as follows: ionization voltage +2.0 kV, ion transfer tube temperature 250 °C, mass range 150-1,500, mass resolution 60,000 at m/z 400, 1 microscan, 500 ms max injection time, and automatic gain control (AGC) with the target value of  $1 \times 10^6$ . Each lysate was analyzed three times (i.e., three analytical replicates).

**Extraction Efficiency of DAM.** For accurate quantification in LC/MS, the extraction efficiencies of DAM were measured from LC/MS analyses of two groups of cell lysate solutions.

Reference Cell Lysate Solutions. These solutions were prepared from redissolved cell lysate extracts and then spiked with both DAM and its internal standard ( $d_a$ -AML), implying 100% extraction efficiency of DAM. First, we prepared cell pellets.  $0.77-3.62 \times 10^6$  cells/mL of cell suspension were aliquoted into 11 portions, and each portion (1 mL cell suspension) was centrifuged to prepare one pellet. The supernatant was discarded. Second, we prepared cell lysate solutions. Each cell pellet was lysed by urea (8 M). Using the above protocols (D. LC/MS), we performed protein precipitation, extraction of DAM, drying, desalting, and redissolution. Third, we spiked both DAM and  $d_4$ -AML into lysate extracts for LC/MS measurements. Each redissolved extract was spiked with different amounts of DAM (with final concentrations of 2.0, 5.0, 7.5, 10.0, 12.5, 15.0, 17.5, 20.0, 25.0, 30.0, and 50.0 nM) but the same amount of  $d_4$ -AML (10.0 nM final concentration). The final volume of each solution is 100  $\mu$ L. The retention time of  $d_4$ -AML and DAM are close, minimizing the difference of coeluted matrix components on LC/MS quantification. 99 Last, we conducted LC/MS measurements. Without further extraction (i.e., 100% extraction efficiency), these samples were directly used for LC/MS analysis to obtain the relative peak areas of DAM/ $d_4$ -AML.

Cell Lysate Solutions Containing Extracted DAM and Spiked  $d_4$ -AML. To prepare these solutions, extracts were obtained from cell lysates containing DAM, redissolved, and then spiked with  $d_4$ -AML for LC/MS measurements. First, we prepared cell pellets using the same protocols as described above. Second, we prepared DAM-containing solutions of cell lysates. Each cell pellet was lysed using urea (8 M). Different amounts of DAM were added into lysates with a series of final concentrations (i.e., 2.0, 5.0, 7.5, 10.0, 12.5, 15, 17.5, 20.0, 25.0, 30.0, and 50.0 nM). Third, we extracted DAM from cell lysate solutions using cold acetone following the same protocols provided above (D. LC/MS). Fourth, we spiked  $d_4$ -AML (10 nM final concentration) into each redissolved extract. Last, we performed an LC/MS analysis of these samples to acquire the relative peak areas of DAM/ $d_4$ -AML.

Three analytical replicates for each group were measured. The DAM extraction efficiency of DAM (48.5  $\pm$  7.4%) was determined by comparing the ratios of DAM/ $d_4$ -AML obtained from these two groups of samples. This measured

DAM extraction efficiency was used to correct the LC/MS measurement of the average intracellular DAM (i.e., NO).

Data Analysis of Cell Subpopulations. SCMS and LC/ MS raw data were accessed using an Xcalibur 5.0 (Thermo Fisher Scientific). In SCMS experiments, the detection of single cells was confirmed from the appearance of typical cellular species (e.g., PC (34:1), m/z 782.567). The LC/MS retention time was measured as 21.47 and 21.81 min for DAM and  $d_4$ -AML, respectively. The peak areas of both DAM and d<sub>4</sub>-AML were exported from Xcaliber and imported into Microsoft Excel for quantification. D > 2 Ashman's criterion was used to confirm the presence of subpopulations with normal distributions in SNP (exogenous NO) treatment groups. Gamma distribution functions were used to fit results from DOX (endogenous NO) treatment groups. The dip test was used to determine if subpopulations exist. All fittings were generated by a homemade Python script (Supporting Information).

### ■ RESULTS AND DISCUSSION

Calibration Curves of SCMS Experiments. During SCMS measurements, intensive isobaric background ions (ranging from m/z 407.1040 to 407.2090) interfered with the isolation and detection of the target ion DAM ([DAM +  $H^+$ , m/z 407.1325, Figures S3 and S4). These interfering ions significantly affected the direct quantification of NO (i.e., DAM) in a single cell using MS1. In contrast, our experiments showed that the MS/MS spectra of the interfering ions were significantly different from those of [DAM + H]<sup>+</sup> (Figure S3), indicating that DAM quantification can be performed using MS/MS to eliminate the influence of interfering ions. Due to the unavailability of isotopically DAM compounds, oxasulfuron (OXF) was chosen as the internal standard of DAM. This is because  $[OXF + H]^+$  (m/z 407.1020) can be coisolated with  $[DAM + H]^+$  (m/z 407.1325) for MS/MS analysis, whereas their fragments are significantly different (Figures S5 and S6). Another benefit of using MS/MS quantification is that mass spectra with a cleaner background can be obtained (Figure S5), resulting in improved detection sensitivity due to an increased signal-to-noise ratio. 100 Our experiments indicated that using the Single-probe SCMS setup, the limit of detection for DAM is 0.2 and 0.05 nM in MS1 and MS/MS measurements, respectively. MS/MS calibrations are detailed in the Supporting Information.

Calibration Curve of LC/MS Experiments. LC/MS experiments were conducted to obtain the average NO amounts in the single cells. To mimic the matrix effect in LC-MS experiments, a cell lysate was used to prepare solutions containing the standard compounds. Briefly, cell lysate was dissolved in the solvent [MeOH  $(20\%)/H_2O$  (80%)with 0.1% FA]. Cell lysate aliquots were spiked with different amounts of DAM (final concentrations: 0.2, 0.5, 1.0, 2.0, 5.0, 10, and 20 nM) but a fixed amount of  $d_4$ -AML (final concentration: 100 nM). Each sample was analyzed with three analytical replicates. Because all interfering species were eliminated by LC separation, MS1 spectra were used to construct the LC/MS calibration curve (Supporting Information). All experiments were performed using the same instrument settings on the same day. For accurate quantification, the extraction efficiencies of DAM from cell lysates were measured (E. Extraction efficiency of DAM). This measured extraction efficiency (48.5  $\pm$  7.4%) was then used to

correct the LC/MS quantification of average intracellular DAM (i.e., NO) (Table 1).

Table 1. Amounts of NO in Single Cells Were Measured Using SCMS and LC/MS Methods

cell group	treatment concentrations <sup>a</sup>	SCMS amount (amol)	$n^b$	LC/MS amount (amol)
SNP-L	0.25 mM	$23.4 \pm 13.9$	41	$0.82 \pm 0.10$
SNP-M	1.0 mM	$25.3 \pm 22.7$	48	$1.92 \pm 0.12$
SNP-H	4.0 mM	$60.4 \pm 67.0$	51	$5.47 \pm 0.41$
DOX-L	$0.75~\mu\mathrm{M}$	$36.8 \pm 40.5$	94	$2.91 \pm 0.20$
DOX-M	$2.0~\mu\mathrm{M}$	$46.6 \pm 48.0$	41	$4.05 \pm 0.17$
DOX-H	$4.0~\mu\mathrm{M}$	$61.7 \pm 93.9$	60	$10.72 \pm 0.48$

<sup>a</sup>Cells were treated by SNP (sodium nitroprusside) or DOX (doxorubicin) for 24 h.  $^bn$  indicates the number of single cells measured in each SCMS experiment.

SCMS Quantification of Exogenous and Endogenous NO in Single Cells. Cells were attached to the microwell glass chip through incubation (Figure 1B). Using similar experimental protocols reported in our previous studies, so only microwells containing one cell were measured using the Single-probe SCMS setup. 1.0  $\mu$ M OXF (the internal standard for DAM) was added to the sampling solvent, of which the flow rate was recorded for the analysis of each cell. Based on the calibration curve (Figure S1), the integrated intensities of major fragments of DAM and OXF were used to quantify DAM in each cell.

In SCMS studies of exogenous NO, AML-treated cells were rinsed and then incubated (for 24 h) in a medium containing three different concentrations of sodium nitroprusside (SNP), i.e., low (SNP-L, 0.25 mM), medium (SNP-M, 1.0 mM), and high (SNP-H, 4.0 mM). As a NO donor, SNP is absorbed by cells to release NO through reactions with sulfhydryl groups in proteins. 11,12 NO molecules then react with intracellular AML and produce DAM (Figure 1A). Cells (n = 41-51) in each group were analyzed using the Single-probe SCMS technique. Our experimental results indicated broad distributions of intracellular NO of cells in all three groups, very likely due to cell heterogeneity (Figure 2A). Similarly, heterogeneous anticancer drug uptake in single cells has been observed in our previous studies. 86,87 The average NO amounts in SNP-L, SNP-M, and SNP-H groups are  $23.4 \pm 13.9$ ,  $25.3 \pm 22.7$ , and  $60.4 \pm 67.0$  amol  $(10^{-18} \text{ mol})/\text{cell}$ , respectively (Table 1). Although there is no significant difference in results between the SNP-L and SNP-M treatment groups (t-test, p > 0.05), higher concentration treatment in the SNP-H group

significantly boosted NO production compared to the SNP-L treatment group (t-test, p < 0.05) (Figure 2A).

In the studies of endogenous NO in single cells, AMLtreated cells were rinsed and then incubated in a medium containing the anticancer drug doxorubicin (DOX), which stimulated the production of NO. As a transient paracrine and autocrine signaling molecule, NO plays important functions in the cellular and intercellular drug response. 101,102 Previous studies proved that the NO level in cells can be increased by DOX treatment due to elevated NOS activities. 13-15 To evaluate the relationship between the DOX concentration and the amount of endogenous NO in cells, HCT-116 cells were treated (for 24 h) with DOX at three different concentrations, i.e., low (DOX-L, 0.75  $\mu$ M), medium (DOX-M, 2.0  $\mu$ M), and high (DOX-H, 4.0  $\mu$ M). Cells (n = 41-94) in each group were then analyzed using the Single-probe SCMS technique. Broad distributions of intracellular NO amounts were observed (Figure 2B). The measured NO amounts in single cells from the DOX-L, DOX-M, and DOX-H groups are  $36.8 \pm 40.5$ ,  $46.6 \pm 48.0$ , and  $61.7 \pm 93.9$  amol/cell, respectively (Table 1). Similar to results obtained from the exogenous NO treatment, there is no significant difference between the DOX-L and DOX-M treatments (t-test, p < 0.05), but a higher concentration of DOX in the DOX-H group significantly stimulated NO production compared to the DOX-L group (ttest, p < 0.05) (Figure 2B).

The mean values  $(23.4-61.7 \times 10^{-18} \text{ mol/cell})$  of NO abundances in single cells obtained from our experiments may not be fairly compared with previously reported results. In fact, intracellular NO abundances can significantly vary for different cell systems. For example, the amounts of NO in RAW 264.7 cells, which were stimulated by lipopolysaccharide (LPS) to produce NO, were reported as  $1.4-2.1 \times 10^{-16}$  mol/cell,  $^{103,104}$ whereas PC-12 cells exhibited a broad range of  $4 \times 10^{-18}$  to 4.5  $\times 10^{-14}$  mol/cell. <sup>52,105</sup> To the best of our knowledge, there are no reported studies of the same cell system used in our current work. Therefore, a direct comparison at the single-cell level cannot be performed. It has been reported that AML treatment can stimulate the production of cellular NO. However, in our control experiments, we were unable to detect DAM in single cells only treated by AML, which can scavenge NO and produce DAM. Our results indicated that the amounts of NO, if any, induced by AML in HCT-116 cells were below the detection limit of our Single-probe SCMS technique.

Subpopulation Analysis of NO Quantities in Single Cells. Cell heterogeneity has been studied at different levels, such as transcriptomics and metabolomics, using statistical

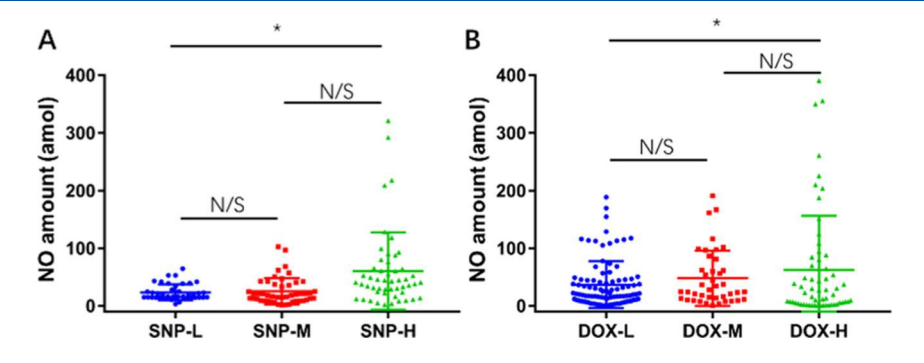


**Figure 2.** Box plots indicating (A) exogenous (SNP treated, 24 h) and (B) endogenous (DOX treated, 24 h) NO amounts (amol) in single cells. (\*: p < 0.05, N/S: no significant difference).

tools. Cells' subpopulations can be evaluated based on the overall molecular profiles. For example, we have previously developed a tool, SinChat\_MS, to quantify cell subpopulations based on their global metabolites in single cells. This tool can be also used to prioritize metabolite biomarkers of cell subpopulations and correct batch effects in SCMS studies. Cell subpopulation analysis can also be performed using individual cellular species. For example, Vertes et al. used gamma and normal distribution functions to fit the intensity distributions of multiple molecules (e.g., malate and ascorbate) in *E. densa* epidermal cells and *G. max*-infected root nodule cells and obtained subpopulations. 106

In the current studies, we investigated subpopulations of cells, which reflect cells containing different amounts of NO, by fitting the distributions of the NO amounts in single cells. We evaluated different distribution functions, and we discovered that normal and gamma distribution functions provided the best fittings for endogenous and exogenous NO groups, respectively (Figure 3). Our fitting results also indicate

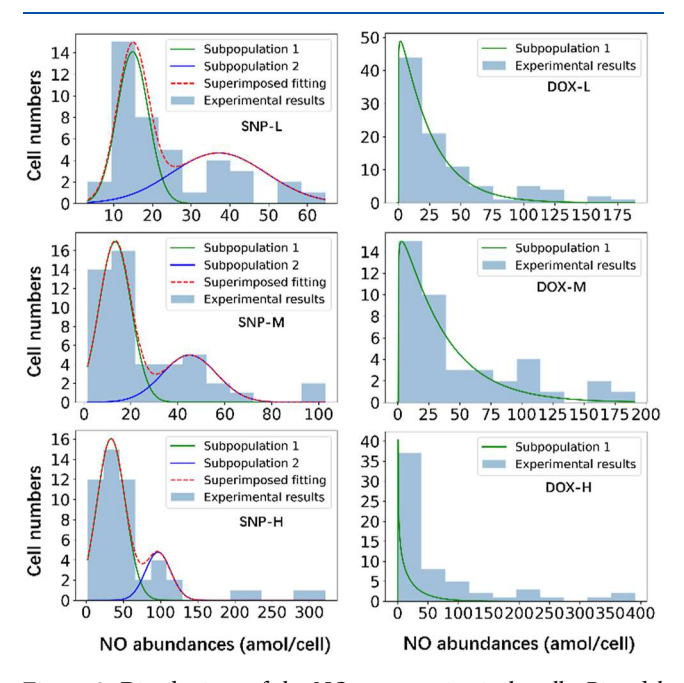


Figure 3. Distributions of the NO amounts in single cells. Bimodal (normal) distributions were observed in exogenous NO groups (SNP treatment, left panel). Unimodal (gamma) distributions were observed in endogenous NO groups (DOX treatment, right panel).

that there are two subpopulations of cells in all three exogenous NO treatment groups (Figure 3, left panel). We further confirmed the presence of two subpopulations using the D > 2 Ashmans's criterion (Supporting Information). 106,107 The  $D_{12}$  values for subpopulations 1 and 2 are 3.67, 4.00, and 2.31 for the SNP-L, SNP-M, and SNP-H treatment groups, respectively. The t-test results indicate that these two subpopulations of cells contain significantly different (p < 0.05) amounts of NO. The average amounts of NO in single cells from two subpopulations are summarized in Table 2. Compared with the results shown in Table 1, grouping cells into two subpopulations leads to significantly reduced standard deviations. For cells containing endogenous NO, we observed one population (gamma distributions) in all three treatment groups (Figure 3, right panel). To determine if there are multimodal distributions, a dip test has been performed,

Table 2. Amount of Exogenous NO in Single Cells in Two Subpopulations

cell groups	subpopulation 1 (amol)	subpopulation 2 (amol)
SNP-L	$15.7 \pm 4.8$	$40.5 \pm 11.6$
SNP-M	$13.3 \pm 6.9$	$52.3 \pm 22.3$
SNP-H	$33.6 \pm 19.3$	$96.7 \pm 18.2$

yielding no clear evidence of multimodality (Supporting Information). Our results indicate that exogenous and endogenous treatment conditions resulted in different modalities of distributions of NO amounts in single cells, likely due to different levels of toxicities between SNP and DOX. Although there is no reported assessment of SNP toxicity to HCT-116 cells, our cell culture experiments indicated that, compared with cells in normal growing conditions, cell growth was not obviously inhibited by SNP at all three concentrations. Thus, more heterogeneous cells were analyzed in our SCMS experiment. In contrast, DOX is a potent anticancer drug (IC<sub>50</sub> =  $0.96 \pm 0.02 \,\mu\text{M}$  (72 h) for HCT-116 cells). Under our DOX treatment conditions (0.75, 2.0, or 4.0  $\mu$ M for 24 h), cells with relatively low drug resistance can be largely eliminated from SCMS measurements, resulting in less cell heterogeneity. Although broad distributions of intracellular NO amounts were observed in the previous studies, which were primarily based on fluorescence microscopy techniques, further investigation of cell subpopulations was not conducted. 52,104,105,109 The difference in cell heterogeneity can be potentially validated using other single-cell analysis techniques such as single-cell RNA sequencing. However, these studies are beyond the scope of the current studies.

LC/MS Quantification of NO in Cell Lysates. In the comparative studies, LC/MS analyses of cell lysates, which were prepared using cells under treatment conditions that are the same as those in SCMS studies, were carried out to obtain the average quantities of NO in single cells. The total amounts of NO in cell lysates were calculated using the calibration curve (Figure 2B), with the correction of the extraction efficiencies. The average NO amounts in single cells were then calculated on the basis of the total number of cells in each sample (Table S1). First, LC/MS results exhibit a clear trend: the intracellular NO amounts increase as the treatment concentrations of SNP and DOX increase. This trend cannot be clearly observed in our SCMS measurements of cells treated by low and medium concentrations of SNP and DOX, likely due to a relatively small difference in intracellular NO abundances and cell heterogeneity. Second, the mean values of our SCMS results  $(23.4-61.7 \times 10^{-18} \text{ mol/cell})$  are generally higher than those from our LC/MS measurements (0.9–10.7  $\times$  10<sup>-18</sup> mol/cell). This difference is likely due to cell heterogeneity in SCMS experiments, which resulted in large standard deviations, and potential DAM loss in multiple sample preparation steps in LC/MS experiments such as trypsin detachment and several rounds of cell washing and centrifugation. During these procedures, intracellular DAM might be lost due to cell rupture and diffusion across the cell membrane, whereas the internal standard ( $d_4$ -AML) cannot be added in these steps to compensate for this loss. SCMS involves minimal sample preparation, which reduces the change of DAM loss between the sample preparation and measurement. Sample loss during LC/MS sample preparation can likely result in small amounts of DAM compared with those in SCMS experiments. Similar trends have been observed in our previous studies of

intracellular anticancer drug compounds. <sup>86</sup> Third, our LC/MS results are lower than that ( $\sim$ 0.6  $\times$  10<sup>-16</sup> mol/cell) in LPS-stimulated RAW 264.7 cells measured by LC/MS methods, <sup>22</sup> likely due to the intrinsic differences between these two cell lines and treatment conditions.

## CONCLUSIONS

We combined the quantitative Single-probe SCMS technique with chemical reactions, in which AML quantitatively reacts with intracellular NO to produce DAM, to quantify NO amounts in live single cells. Two different compounds [i.e., sodium nitroprusside (SNP) and doxorubicin (DOX)] with different treatment concentrations were used to produce exogenous (by SNP) or endogenous (by DOX) NO. Under all treatment conditions, intracellular NO amounts exhibited heterogeneous distributions. The distributions of NO amounts in single cells were analyzed, and results indicated that two subpopulations of cells were present in all exogenous NO treatment groups, whereas only one population was discovered in each endogenous NO treatment group. This difference can be potentially attributed to different toxicities between SNP and DOX. Comparison studies of lysates of cells treated under the same conditions were performed using the LC/MS method. The mean values obtained from single cells were significantly higher than those measured from bulk samples, likely due to cell heterogeneity and potential drug compound loss during cell lysate preparation. The technique reported in the current study is applicable to quantify NO in many other types of cells. However, this technique has a relatively low throughput due to manual selection and analysis of single cells. This drawback can be potentially solved by developing highthroughput SCMS methods. In addition, this method is largely limited to analyzing adherent cells, whereas measuring nonadherent cells requires additional instrument modification. 90,110 The strategy of combining SCMS techniques and chemical reactions can be potentially further developed to study other cellular species of interest.

## ASSOCIATED CONTENT

# Supporting Information

The Supporting Information is available free of charge at https://pubs.acs.org/doi/10.1021/acs.analchem.3c04393.

Mass spectra (DAM, OXF, and interfering ions), supporting table, and codes (Python and R) for data fitting (PDF)

### AUTHOR INFORMATION

## **Corresponding Author**

Zhibo Yang — Department of Chemistry and Biochemistry, University of Oklahoma, Norman, Oklahoma 73019, United States; orcid.org/0000-0003-0370-7450; Email: Zhibo.Yang@ou.edu

#### Authors

Yunpeng Lan — Department of Chemistry and Biochemistry, University of Oklahoma, Norman, Oklahoma 73019, United States

Xingxiu Chen — Department of Chemistry and Biochemistry, University of Oklahoma, Norman, Oklahoma 73019, United States

Complete contact information is available at: https://pubs.acs.org/10.1021/acs.analchem.3c04393

#### Notes

The authors declare no competing financial interest.

## ACKNOWLEDGMENTS

This work was supported by funds from the National Science Foundation (2305182), the National Institutes of Health (1R01AI177469), the Research Council of the University of Oklahoma Norman Campus, and the University of Oklahoma's Office of the Vice President for Research and Partnerships.

#### REFERENCES

- (1) Bruckdorfer, R. Mol. Aspects Med. 2005, 26 (1-2), 3-31.
- (2) Garthwaite, J.; Boulton, C. Annu. Rev. Physiol. 1995, 57 (1), 683-706.
- (3) Cary, S. P.; Winger, J. A.; Derbyshire, E. R.; Marletta, M. A. *Trends Biochem. Sci.* **2006**, *31* (4), 231–239.
- (4) Naseem, K. M. Mol. Aspects Med. 2005, 26 (1-2), 33-65.
- (5) Loscalzo, J.; Welch, G. Prog. Cardiovasc. Dis. 1995, 38 (2), 87–04.
- (6) Jota Baptista, C. V.; Faustino-Rocha, A. I.; Oliveira, P. A. *Pharmacology* **2021**, *106* (7–8), 356–368.
- (7) SoRelle, R. Circulation 1998, 98 (22), 2365-2366.
- (8) Hermann, M.; Flammer, A.; Lüscher, T. F. J. Clin. Hypertens. **2006**, 8, 17–29.
- (9) Carnicer, R.; Crabtree, M. J.; Sivakumaran, V.; Casadei, B.; Kass, D. A. Antioxid. Redox Signaling 2013, 18 (9), 1078–1099.
- (10) Divakaran, S.; Loscalzo, J. J. Am. Coll. Cardiol. 2017, 70 (19), 2393–2410.
- (11) Curry, S. C.; Spyres, M. B. Sodium Nitroprusside. In *Critical Care Toxicology: Diagnosis and Management of the Critically Poisoned Patient*; Brent, J., Burkhart, K., Dargan, P., Hatten, B., Megarbane, B., Palmer, R., White, J., Eds.; Springer International Publishing, 2017; pp 843–850.
- (12) Holme, M. R.; Sharman, T. Sodium Nitroprusside; StatPearls Publishing, 2020.
- (13) Sayed-Ahmed, M. M.; Khattab, M. M.; Gad, M. Z.; Osman, A. M. M. *Pharmacol. Toxicol.* **2001**, 89 (3), 140–144.
- (14) Salaroglio, I. C.; Gazzano, E.; Abdullrahman, A.; Mungo, E.; Castella, B.; Abd-elrahman, G. E. F. A.-e.; Massaia, M.; Donadelli, M.; Rubinstein, M.; Riganti, C.; et al. *J. Exp. Clin. Cancer Res.* **2018**, *37*, 286
- (15) Aldieri, E.; Bergandi, L.; Riganti, C.; Costamagna, C.; Bosia, A.; Ghigo, D. Toxicol. Appl. Pharmacol. 2002, 185 (2), 85–90.
- (16) Taylor-Robinson, A. W.; Liew, F. Y.; Severn, A.; Xu, D.; McSorley, S. J.; Garside, P.; Padron, J.; Phillips, R. S. Eur. J. Immunol. 1994, 24 (4), 980–984.
- (17) Bogdan, C. Nat. Immunol. 2001, 2 (10), 907-916.
- (18) Bogdan, C. The function of nitric oxide in the immune system. *Nitric Oxide*; Springer, 2000; pp 443–492.
- (19) Tripathi, P.; Tripathi, P.; Kashyap, L.; Singh, V. FEMS Immunol. Med. Microbiol. 2007, 51 (3), 443-452.
- (20) Ye, X.; Rubakhin, S. S.; Sweedler, J. V. Analyst 2008, 133 (4), 423-433.
- (21) Hu, Y.; Xiang, J.; Su, L.; Tang, X. J. Int. Med. Res. 2020, 48 (2), 030006052090598.
- (22) Zhong, Z.-J.; Yao, Z.-P.; Shi, Z.-Q.; Liu, Y.-D.; Liu, L.-F.; Xin, G.-Z. Anal. Chem. **2021**, 93 (24), 8536–8543.
- (23) Singh, S.; Gupta, A. K. Cancer Chemother. Pharmacol. 2011, 67, 1211–1224.
- (24) Mocellin, S. Curr. Cancer Drug Targets 2009, 9 (2), 214-236.
- (25) Raj, A.; Rifkin, S. A.; Andersen, E.; van Oudenaarden, A. *Nature* **2010**, *463* (7283), 913–918.
- (26) Qian, C.; Yun, Z.; Yao, Y.; Cao, M.; Liu, Q.; Hu, S.; Zhang, S.; Luo, D. Scand. J. Immunol. **2019**, 90 (1), No. e12768.
- (27) Meacham, C. E.; Morrison, S. J. Nature 2013, 501 (7467), 328-337.
- (28) Tang, D. G. Cell Research 2012, 22 (3), 457-472.

- (29) Gay, L.; Baker, A.-M.; Graham, T. A. F1000Research 2016, 5, 238.
- (30) Xie, H.; Li, Y.-T.; Lei, Y.-M.; Liu, Y.-L.; Xiao, M.-M.; Gao, C.; Pang, D.-W.; Huang, W.-H.; Zhang, Z.-Y.; Zhang, G.-J. *Anal. Chem.* **2016**, 88 (22), 11115–11122.
- (31) Archer, S. FASEB J. 1993, 7 (2), 349-360.
- (32) Yao, D.; Vlessidis, A. G.; Evmiridis, N. P. Microchim. Acta 2004, 147, 1–20.
- (33) Hetrick, E. M.; Schoenfisch, M. H. Annu. Rev. Anal. Chem. 2009, 2, 409-433.
- (34) Taha, Z. H. Talanta 2003, 61 (1), 3-10.
- (35) Murphy, M. E.; Noack, E. Nitric oxide assay using hemoglobin method. *Methods in Enzymology*; Elsevier, 1994; Vol. 233, pp 240–250.
- (36) Sun, J.; Zhang, X.; Broderick, M.; Fein, H. Sensors 2003, 3 (8), 276–284.
- (37) Bryan, N. S.; Grisham, M. B. Free Radical Biol. Med. 2007, 43 (5), 645-657.
- (38) Hong, H.; Sun, J.; Cai, W. Free Radical Biol. Med. **2009**, 47 (6), 684–698.
- (39) Woldman, Y. Y.; Eubank, T. D.; Mock, A. J.; Stevens, N. C.; Varadharaj, S.; Turco, J.; Gavrilin, M. A.; Branchini, B. R.; Khramtsov, V. V. Biochem. Biophys. Res. Commun. 2015, 465 (2), 232–238.
- (40) MacArthur, P. H.; Shiva, S.; Gladwin, M. T. J. Chromatogr. B **2007**, 851 (1-2), 93-105.
- (41) Ciszewski, A.; Milczarek, G. Talanta 2003, 61 (1), 11-26.
- (42) Jo, A.; Do, H.; Jhon, G.-J.; Suh, M.; Lee, Y. Anal. Chem. 2011, 83 (21), 8314–8319.
- (43) Tang, L.; Li, Y.; Xie, H.; Shu, Q.; Yang, F.; Liu, Y.-l.; Liang, F.; Wang, H.; Huang, W.; Zhang, G.-J. Sci. Rep. 2017, 7 (1), 6446.
- (44) Trettin, A.; Böhmer, A.; Suchy, M.-T.; Probst, I.; Staerk, U.; Stichtenoth, D. O.; Frölich, J. C.; Tsikas, D. Oxid. Med. Cell. Longevity 2014, 2014, 212576.
- (45) Becker, A.; Ückert, S.; Tsikas, D.; Noack, H.; Stief, C.; Frölich, J. C.; Wolf, G.; Jonas, U. *Urol. Res.* **2000**, 28, 364–369.
- (46) Kiechle, F. L.; Malinski, T. Am. J. Clin. Pathol. 1993, 100 (5), 567–575.
- (47) Hirayama, A.; Nagase, S.; Ueda, A.; Yoh, K.; Oteki, T.; Obara, M.; Takada, K.; Shimozawa, Y.; Aoyagi, K.; Koyama, A. Electron paramagnetic resonance imaging of nitric oxide organ distribution in lipopolysuccaride treated mice. *Guanidino Compounds in Biology and Medicine*; Springer, 2003; pp 63–67.
- (48) Ren, J.; Fung, P.; Chang, C.; Shen, G.; Lu, G.; Chan, F.; Liu, K.; Shen, J. Appl. Magn. Reson. 2007, 32, 243–255.
- (49) Lindermayr, C.; Durner, J. J. Exp. Bot. 2018, 69 (15), 3507–3510.
- (50) Fujii, H.; Wan, X.; Zhong, J.; Berliner, L. J.; Yoshikawa, K. Magn. Reson. Med. 1999, 42 (2), 235–239.
- (51) Liu, G.; Pagel, M. A smart PARACEST MRI contrast agent for nitric oxide detection. *Proceedings of the 14th Annual Meeting of ISMRM*, 2006.
- (52) Yang, Q.; Zhang, X.; Bao, X.; Lu, H.; Zhang, W.; Wu, W.; Miao, H.; Jiao, B. J. Chromatogr. A 2008, 1201 (1), 120–127.
- (53) Sarti, P.; Lendaro, E.; Ippoliti, R.; Bellelli, A.; Benedetti, P. A.; Brunori, M. *FASEB J.* **1999**, *13* (1), 191–197.
- (54) He, Q.; Goshi, E.; Zhou, G. Med. Gas Res. 2019, 9 (4), 192.
- (55) Kind, T.; Tsugawa, H.; Cajka, T.; Ma, Y.; Lai, Z.; Mehta, S. S.; Wohlgemuth, G.; Barupal, D. K.; Showalter, M. R.; Arita, M.; et al. *Mass Spectrom. Rev.* **2018**, *37* (4), 513–532.
- (56) Kim, B.; Araujo, R.; Howard, M.; Magni, R.; Liotta, L. A.; Luchini, A. Expert Rev. Proteomics 2018, 15 (4), 353–366.
- (57) Guzman, N. A.; Blanc, T.; Phillips, T. M. Electrophoresis 2008, 29 (16), 3259-3278.
- (58) Zhang, L.; Vertes, A. Angew. Chem., Int. Ed. 2018, 57 (17), 4466-4477.
- (59) Tajik, M.; Baharfar, M.; Donald, W. A. Trends Biotechnol. 2022, 40 (11), 1374-1392.
- (60) Yang, Y.; Huang, Y.; Wu, J.; Liu, N.; Deng, J.; Luan, T. TrAC, Trends Anal. Chem. 2017, 90, 14–26.

- (61) Yin, L.; Zhang, Z.; Liu, Y.; Gao, Y.; Gu, J. Analyst 2019, 144 (3), 824–845.
- (62) Schober, Y.; Guenther, S.; Spengler, B.; Römpp, A. Anal. Chem. **2012**, 84 (15), 6293–6297.
- (63) Wu, K.; Jia, F.; Zheng, W.; Luo, Q.; Zhao, Y.; Wang, F. *JBIC, J. Biol. Inorg. Chem.* **2017**, *22*, 653–661.
- (64) Zhu, X.; Xu, T.; Peng, C.; Wu, S. Front. Chem. 2022, 9, 782432. (65) Ifa, D. R.; Wu, C.; Ouyang, Z.; Cooks, R. G. Analyst 2010, 135
- (4), 669–681. (66) Soudah, T.; Zoabi, A.; Margulis, K. Mass Spectrom. Rev. 2023, 42 (2), 751–778.
- (67) Roach, P. J.; Laskin, J.; Laskin, A. Analyst **2010**, 135 (9), 2233–2236.
- (68) Hale, O. J.; Cooper, H. J. Anal. Chem. 2021, 93 (10), 4619–4627.
- (69) Li, X.; Hu, H.; Yin, R.; Li, Y.; Sun, X.; Dey, S. K.; Laskin, J. Anal. Chem. **2022**, 94 (27), 9690–9696.
- (70) Mizuno, H.; Tsuyama, N.; Harada, T.; Masujima, T. J. Mass Spectrom. 2008, 43 (12), 1692-1700.
- (71) Tsuyama, N.; Mizuno, H.; Tokunaga, E.; Masujima, T. Anal. Sci. 2008, 24 (5), 559–561.
- (72) Shimizu, T.; Miyakawa, S.; Esaki, T.; Mizuno, H.; Masujima, T.; Koshiba, T.; Seo, M. *Plant Cell Physiol.* **2015**, *56* (7), 1287–1296.
- (73) Pan, N.; Rao, W.; Kothapalli, N. R.; Liu, R.; Burgett, A. W.; Yang, Z. Anal. Chem. 2014, 86 (19), 9376–9380.
- (74) Pan, N.; Rao, W.; Standke, S. J.; Yang, Z. Anal. Chem. 2016, 88 (13), 6812–6819.
- (75) Nguyen, T. D.; Lan, Y.; Kane, S. S.; Haffner, J. J.; Liu, R.; McCall, L.-I.; Yang, Z. Anal. Chem. **2022**, 94 (30), 10567–10572.
- (76) Liu, R.; Pan, N.; Zhu, Y.; Yang, Z. Anal. Chem. 2018, 90 (18), 11078-11085.
- (77) Zhu, Y.; Liu, R.; Yang, Z. Anal. Chim. Acta 2019, 1084, 53-59.
- (78) Nemes, P.; Vertes, A. Anal. Chem. 2007, 79 (21), 8098-8106.
- (79) Meng, Y.; Song, X.; Zare, R. N. Anal. Chem. 2022, 94 (28), 10278-10282.
- (80) Wei, Z.; Xiong, X.; Guo, C.; Si, X.; Zhao, Y.; He, M.; Yang, C.; Xu, W.; Tang, F.; Fang, X.; et al. *Anal. Chem.* **2015**, 87 (22), 11242–11248.
- (81) Zhu, G.; Shao, Y.; Liu, Y.; Pei, T.; Li, L.; Zhang, D.; Guo, G.; Wang, X. TrAC, Trends Anal. Chem. 2021, 143, 116351.
- (82) Gillette, M. A.; Carr, S. A. Nat. Methods **2013**, 10 (1), 28–34.
- (83) Urban, P. L. Philos. Trans. R. Soc., A 2016, 374 (2079), 20150382.
- (84) Liu, R.; Yang, Z. Anal. Chim. Acta 2021, 1143, 124-134.
- (85) Ali, A.; Abouleila, Y.; Amer, S.; Furushima, R.; Emara, S.; Equis, S.; Cotte, Y.; Masujima, T. *Anal. Sci.* **2016**, *32* (2), 125–127.
- (86) Pan, N.; Standke, S. J.; Kothapalli, N. R.; Sun, M.; Bensen, R. C.; Burgett, A. W.; Yang, Z. *Anal. Chem.* **2019**, *91* (14), 9018–9024.
- (87) Bensen, R. C.; Standke, S. J.; Colby, D. H.; Kothapalli, N. R.; Le-McClain, A. T.; Patten, M. A.; Tripathi, A.; Heinlen, J. E.; Yang, Z.; Burgett, A. W. ACS Pharmacol. Transl. Sci. 2021, 4 (1), 96–100.
- (88) Rubakhin, S. S.; Sweedler, J. V. Anal. Chem. 2008, 80 (18), 7128-7136.
- (89) Yin, R.; Prabhakaran, V.; Laskin, J. Anal. Chem. 2018, 90 (13), 7937–7945.
- (90) Standke, S. J.; Colby, D. H.; Bensen, R. C.; Burgett, A. W.; Yang, Z. J. Visualized Exp. 2019, 148, No. e59875.
- (91) Liu, R.; Sun, M.; Zhang, G.; Lan, Y.; Yang, Z. Anal. Chim. Acta 2019, 1092, 42–48.
- (92) Liu, R.; Li, J.; Lan, Y.; Nguyen, T. D.; Chen, Y. A.; Yang, Z. Anal. Chem. 2023, 95 (18), 7127-7133.
- (93) Itoh, T.; Nagata, K.; Matsuya, Y.; Miyazaki, M.; Ohsawa, A. J. Org. Chem. 1997, 62 (11), 3582–3585.
- (94) Ma, S.; Fang, D.-C.; Ning, B.; Li, M.; He, L.; Gong, B. Chem. Commun. 2014, 50 (49), 6475–6478.
- (95) Gao, C.; Lin, L.; Sun, W.; Tan, Z.-L.; Huang, J.-R.; He, L.; Lu, Z.-L. *Talanta* **2018**, *176*, 382–388.
- (96) Li, H.; Zhang, D.; Gao, M.; Huang, L.; Tang, L.; Li, Z.; Chen, X.; Zhang, X. Chem. Sci. 2017, 8 (3), 2199–2203.

- (97) Zhu, Y.; Wang, F.; Li, Q.; Zhu, M.; Du, A.; Tang, W.; Chen, W. Drug Metab. Dispos. **2014**, 42 (2), 245–249.
- (98) Zhu, Y.; Wang, W.; Yang, Z. Anal. Chem. 2020, 92 (16), 11380-11387.
- (99) Panuwet, P.; Hunter, R. E., Jr.; D'Souza, P. E.; Chen, X.; Radford, S. A.; Cohen, J. R.; Marder, M. E.; Kartavenka, K.; Ryan, P. B.; Barr, D. B. *Crit. Rev. Anal. Chem.* **2016**, *46* (2), 93–105.
- (100) Xiao, J. F.; Zhou, B.; Ressom, H. W. TrAC, Trends Anal. Chem. **2012**, 32, 1–14.
- (101) Balligand, J.-L.; Cannon, P. J. Arterioscler., Thromb., Vasc. Biol. 1997, 17 (10), 1846–1858.
- (102) Shah, A. M.; MacCarthy, P. A. Pharmacol. Ther. **2000**, 86 (1), 49–86.
- (103) Yao, H.-W.; Guo, X.-F.; Wang, H. Anal. Chem. 2020, 92 (17), 11904–11911.
- (104) Zhang, Z.-X.; Guo, X.-F.; Wang, H.; Zhang, H.-S. Anal. Chem. **2015**, 87 (7), 3989–3995.
- (105) Li, L.; Li, Q.; Chen, P.; Li, Z.; Chen, Z.; Tang, B. Anal. Chem. **2016**, 88 (1), 930–936.
- (106) Stopka, S. A.; Khattar, R.; Agtuca, B. J.; Anderton, C. R.; Paša-Tolić, L.; Stacey, G.; Vertes, A. Front. Plant Sci. 2018, 9, 1646.
- (107) Ashman, K. A.; Bird, C. M.; Zepf, S. E. Astron. J. 1994, 108, 2348-2361.
- (108) Khaleel, S. A.; Al-Abd, A. M.; Ali, A. A.; Abdel-Naim, A. B. Sci. Rep. **2016**, 6 (1), 36855.
- (109) Mainz, E. R.; Gunasekara, D. B.; Caruso, G.; Jensen, D. T.; Hulvey, M. K.; Fracassi da Silva, J. A.; Metto, E. C.; Culbertson, A. H.; Culbertson, C. T.; Lunte, S. M. Anal. Methods **2012**, 4 (2), 414–420.
- (110) Standke, S. J.; Colby, D. H.; Bensen, R. C.; Burgett, A. W. G.; Yang, Z. Anal. Chem. **2019**, *91* (3), 1738–1742.